6. B. N. Krivosheev, M. P. Kukharskii, and V. D. Portnov, Tr. Mosk. Energ. Inst., No. 448, 32-35 (1980).
7. Y. Ohtsuka, W. Nakayama, and T. Yoshikava, Trans. Jpn. Soc. Mech. Eng., **B50**, No. 457, 2162-2168 (1984).
8. D. A. Labuntsov, Tr. Mosk. Energ. Inst., No. 63, 79-84 (1965).
9. M. G. Semena and Yu. A. Khmelev, Inzh.-Fiz. Zh., **43**, No. 5, 766-774 (1982).

FEATURES OF THE BREAKUP OF JETS OF A LOW-VISCOSITY LIQUID IN A SUBSONIC ENTRAINING FLOW OF GAS

M. E. Rudyak

UDC 532.529

The results of electrocontact measurements are used as a basis for examining the mechanisms (variants) of the breakup of a liquid jet and a dense atomizing jet. The deformational scheme of breakup in an entraining subsonic gas flow is generalized.

In the combustion of liquid fuel, a common practice is to inject a jet of the fuel at an angle into a subsonic flow of cold or heated oxidizing gas. The breakup of the jet is one of the primary acts of mixture formation and ultimately determines the dynamics of the combustion process [1, 2].

The breakup of drops has been examined in detail in the literature [1-10]. The atomization of jets by a supersonic entraining flow was described in [11-18]. Information on the breakup of jets injected at an angle to a subsonic flow was presented in [19-27]. These studies examined the mechanisms (variants) of jet breakup only as a means of explaining and approximating the results of measurements. At the same time, the subject of the mechanisms responsible for the disintegration of jets is of theoretical and, in particular, practical interest. For example, the gradual breakup of a jet [20-22] ensures the supply of fuel to the mixing zone. When the flame is stabilized on the surface of this zone, this situation leads to combination of the processes of mixing and combustion. The flame stabilization phenomenon itself is intimately connected with the breakup of the jet and is employed to provide for special regimes of operation of mixers [22, 26]. The catastrophic breakup of drops [2, 8, 9] or jets [13, 14, 23, 27, 28] contracts the mixing region and elevates its quality [27, 28]. Atomizing with the "stripping" of the surface layer of the liquid yields the finest droplets, which form a nearly homogeneous mixture with the gas [1, 2, 7, 8, 11]. By a variant of breakup, we mean the method by which the flow acts on the jet: "stripping" of a liquid film, excitation and destruction of waves, etc. The act of the separation of a drop from the body of a jet (ligament mechanism) was studied in [29, 30] and is not examined here.

The jet has an integral core which breaks up either gradually, as the jet enters the flow, or suddenly — in the case of catastrophic disintegration [20-23, 27, 28]. The mechanism of the jet's breakup depends on its path (trajectory) and the atomization surface (width of propagation) [20, 21, 25]. The inverse dependence of the degree of penetration of the jet on its breakup — substantiated theoretically in [12] — can be proven only by experiment. The electrocontact method is most informative in this regard, making it possible to determine the jet breakup function $f_b = R_j/R_0$ from the orifice to the point of disintegration of the core for any core trajectory (Fig. 1). The breakup function can be represented in the form

$$f_b = \frac{1}{l_e} \int \frac{F_0}{F} \, dl_e,$$

since

Leningrad Mechanical Institute. Translated from Inzhenerno-Fizicheskii Zhurnal, Vol. 60, No. 1, pp. 24-32, January, 1991. Original article submitted October 3, 1989.

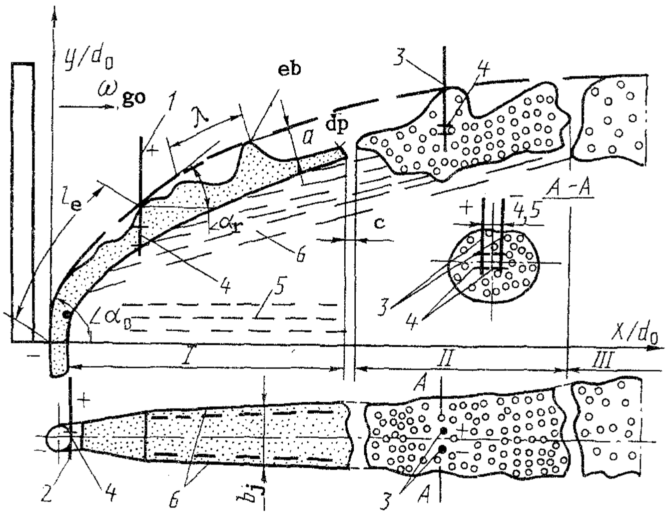

Fig. 1. Electrocontact measurements in a jet: I) core of jet; II) dense ("rigid") spray; III) gas—liquid flow (assimilation of spray); DP) jet disintegration point; D) flow discontinuity; EB) external boundary of jet; 1) probe for jet core; 2) probe for measurements near the orifice; 3) two-electrode probes for spray; 4) electrocontact areas of probes; 5) flow of mass from orifice; 6) "tails" of the jet.

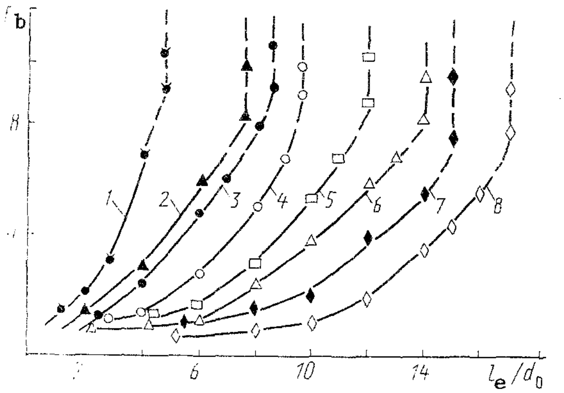

Fig. 2

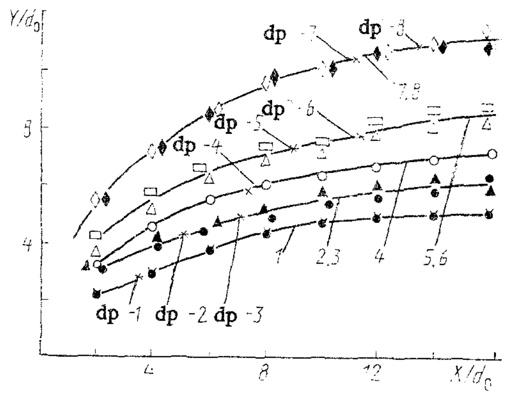

Fig. 3

Fig. 2. Jet breakup functions (the first number denotes φ; the second number denotes ω_{g0}, m/sec; the third number denotes ω_{q0}, m/sec): 1) 0.8/100/13; 2) 0.58/100/15.5; 3) 0.6/55/7.5; 4) 0.45/70/12.5; 5) 0.27/70/16; 6) 0.25/45/10.5; 7) 0.13;80/26; 8) 0.13/60/19.5.

Fig. 3. Trajectories of the external boundaries of jets (the notation is the same as in Fig. 2); DP) core disintegration point.

$$R_0 = \rho'_q \frac{l_e}{F_0}\ ;\ R_j = \rho'_q \int \frac{dl_e}{F}\ .$$

As was shown in [21], the breakup function makes it possible to find the relative cross-sectional area of the jet that can be broken up by a gas flow:

$$\frac{F}{F_0} = l_e \frac{d}{dl_e}\left(\frac{R_j}{R_0}\right) + \frac{R_j}{R_0}$$

as well as the fraction of liquid mass entrained from its surface, $\Delta M = 1 - (F/F_0)$, when there is a correlation between f_b and the simplex normalizing the breakup.

TABLE 1. Parameters of Waves on the Front Surface of the Jet

No. of expt.	φ	$\omega_{г0}$, m/sec	$\frac{a}{d_0}$	$\frac{\lambda}{d_0}$	No. of curves in Figs. 2, 3	No. of expt.	φ	$\omega_{г0}$, м/с	$\frac{a}{d_0}$	$\frac{\lambda}{d_0}$	No. of curves in Figs. 2,3
1	0,8	100	1,0 1,4 1,8	2,0 2,5	1	6	0,25	45	0,2 0,3 0,4	1,1 1,3	6
2	0,58	100	0,7 0,9 1,1	1,6 2,0	2	7	0,13	80	0,4 0,5 0,7 0,9	1,5 2,2 3,2	7
3	0,6	55	0,35 0,42 0,5	1,2 1,4	3	8	0,13	60	0,45 0,75 0,82 0,95	1,8 2,0 2,2	8
4	0,45	70	0,38 0,46 0,55	1,5 1,7	4	9	0,15	100	0,7 0,9 1,1 1,2	1,9 2,2 3,5	—
5	0,27	70	0,25 0,35 0,5 0,6	0,8 1,1 1,5	5	10	0,13	40	0,35 0,45 0,55	1,1 1,3	—

Note. The values of f_b were not determined in experiments Nos. 9 and 10.

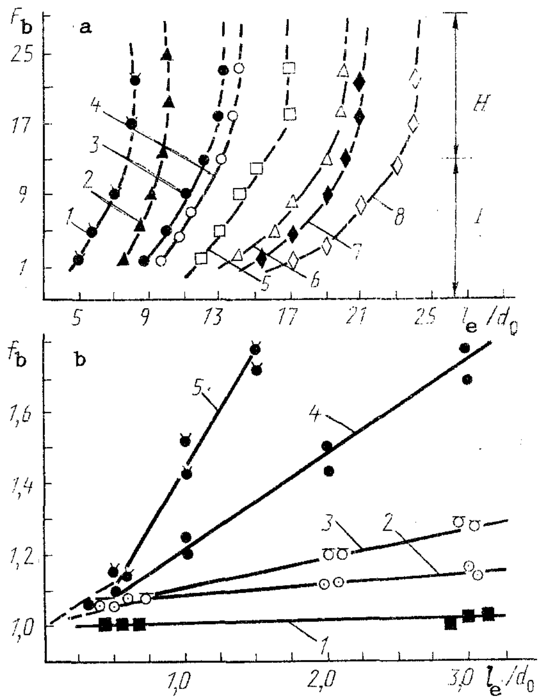

Fig. 4. Breakdown functions for the final and initial sections of a jet: a) breakdown function of a "rigid" spray (the notation is the same as in Fig. 2); I) region of disintegration of the "rigid" spray; II) gas—liquid flow (assimilation of the spray; $F_b \to \infty$); b) breakdown function of the jet next to the mouth (the first number denotes φ; the second number denotes ω_{g0}, m/sec; the third number denotes ω_{q0}, m/sec): 1) discharge without an entraining flow, ω_{q0} = 20 m/sec; 2) 0.06/50/24; 3) 0.05/100/53; 4) 0.6/55/7.5; 5) 0.8/100/13.

The measurements were made with a miniature needle-type probe by the method described in [21-25]. The trajectories of the external boundaries and features of their structure were determined by means of spark photography and streak photography with an exposure of (10^{-5}-10^{-6}) sec. Each point in Figs. 2 and 3 is the result of averaging several tests, each involving the taking of 8-10 spark photographs and the same number of measurements of f_b. The ratio of the dynamic head of the gas to the dynamic head of the liquid $\varphi = \rho_g\omega_{g0}^2/\rho_q\omega_{q0}^2$ was changed both as a result of ω_{g0} and as a result of ω_{q0} at ρ_g/ρ_q = const. The diameter of the mouth of the jet d_0 was equal to 2.01 mm; $\angle\alpha_0 = 90°$; $(l/d_0)_q = 3.5$; the values of p and T for the air flow were 1.2 MPa and 280 K. The water jet was atomized in an entraining submerged flow 35 mm in diameter. The use of water did not distort the mechanisms of jet disintegration [15, 16] or the results of the electrocontact measurements. Thus, the setup just described is suitable for a wide range of low-viscosity fuels.

We can note the following on the basis of the tests. Jets with the same trajectories (curves 2 and 3, 5 and 6, and 7 and 8 in Fig. 3) have different values of f_b (see Fig. 2). The existence of different f_b for the same trajectories can be attributed to the dependence of the penetration on the simplex φ [24] and the large effect of ω_{g0} on the breakup compared to the effect of ω_{q0} [21]. The breakup function of jets whose trajectories are fairly close together — such as 1 and 2, 3; 4 and 5, 6 (Fig. 3) — differ by a factor of 1.5-3. According to the data in [21], this corresponds to a change in ΔM from 0.4 to 0.9. Thus, the penetration of the jet into the flow does not depend on the degree of its disintegration, at least at $\varphi \geq 0.1$. The function f_b also shows that, first of all, the rate of disintegration is variable. Secondly, the breakup of the core, occurring at f_b = 7-8 ($\Delta M \approx 0.95$) [21], completes the atomization process, rather than preceding it. It follows from this that the model in [12], based on the uniform entrainment of mass from a surface covered by capillary waves or acceleration waves, is not representative of the actual pattern of events occurring in the given case. The same can be said of the Schetz model [13-15] for supersonic flow, in which the jet is broken up into "fragments" by a large-amplitude wave without preliminary entrainment. However, the windward side of the jet — clearly recorded by photographing and filming — is unstable: waves having the parameters shown in Table 1 are generated on this side. Three or four such waves are created, the amplitude and length of the waves increasing as the breakup point is approached (and sometimes after it has been passed). An increase in ω_{g0} always marked the formation of a wave. An increase in φ (an increase in the bending of the core) led to some attenuation of the waves. Then the waves intensified again at $\varphi \geq 0.6$ and $\omega_{g0} > 70$ m/sec. If $\varphi \approx 1.0$ and $\omega_{g0} \geq 100$ m/sec, the breakup was catastrophic [23]. A large-amplitude wave destroyed the body of the jet near the mouth; a mechanism similar to that described in [13-15] was operative in this case.

Evaluation of the nature of the waves that are created requires a knowledge of the dynamics of motion of the jet. We optically recorded discontinuities in the spray below the core disintegration point and found the rate of displacement of the wave crest above this point. It was determined that the acceleration of the jet along the X axis before its breakup was $j_{jx} = (1\text{-}2)\cdot 10^4$ m/sec^2 and occurred due to downstream rotation of the vector of discharge velocity. The acceleration of the spray $j_{ax} = (3\text{-}14)\cdot 10^4$ m/sec^2 and depended on ω_{g0}, the depth of penetration of the jet, and the diameter of the spray. The Bond numbers for the jet were: $B_j = j_{jx}\rho_q d_0^2\sigma^{-1} = (0.5\text{-}1)\cdot 10^3$, with the critical value $B^* = 5\cdot 10^3$ [2, 8]. Thus, catastrophic disintegration of the type associated with Rayleigh—Lamb—Taylor instability is not realized here. For the cases we are examining, the numbers $W_j = \rho_g\omega_{g0}^2 d_0/2\sigma = (0.5\text{-}1.5)\cdot 10^3$. Thus, $W_j \approx B_j \leq 10^3$. This corresponds to the region where the rate of increase in instability of this type is low [2]. Thus, the nature of the waves are evidently of a different character. An analysis of photographs showed that the first wave was generated at $\angle\alpha_r \leq 60\text{-}70°$, i.e., in the region where flexural deformation began. Subsequent intensification of the wave occurred under the influence of the gas flow. It can be assumed that this instability is similar to Kelvin—Helmholtz instability [31]. This assumption is supported by the fact that similar waves are generated on the surface of jets with $\angle\alpha_0 < 90°$ and smaller j_{jx}. The wave processes did not alter the laws governing penetration and disintegration. At the same time, waves on the windward side induce disturbances on other parts of the jet core which are inaccessible to optical recording devices. Thus, the question of the contribution of these waves to disintegration has not yet been fully answered.

The advantages of the electrocontact method are evident form the above and from the data in [20-25, 27]. Progress has been made in improving this method over a long period of time [32-42]. For the simplest cases, electrocontact probing has made it possible to determine the mechanism of disintegration directly by measuring the length of the core or characteristic wave disturbances [32-36]. Studies have been made of the structure of such disturbances in two-phases flows [38, 40], as well as of drop size [39, 41, 42]. Electrocontact measurements in an entraining flow have made it possible to determine the values of f_b, F/F_0, and ΔM [20, 21]. However, they have not permitted definite conclusions to be made as regards the mechanisms responsible for disintegration. This failure can be attributed to the coexistence of an competition between several disintegration variants on each flow section, as well as to the integral nature of the value of f_b itself. Nevertheless, the "randomness of fragmentation" [43] is amenable to a comparative experiment (Figs. 2 and 3) when augmented by information on the structure of the surface of the jet and local mass flows emanating from it.

The breakdown of a slightly curved jet ($\varphi < 0.1$) is normalized by the simplex ε_f [20]:

$$\varepsilon_f = \frac{\delta_f}{d_0} = K \frac{\rho_g}{\rho_q} \left(\frac{V l_e}{\omega_{q0} d_0} \right)^2,$$

where $K = 1/3$ at $\omega_{g0} = \text{const}$; $V = (\omega_{g0}^2 + \omega_{q0}^2)^{\frac{1}{2}}$; δ_f is the maximum displacement of the liquid across the flow during flattening of the jet's contour.

The analogous simplex for a slightly curved jet ($\varphi > 0.1$) has the form [21]:

$$\varepsilon_n = K_n \frac{\rho_g}{\rho_q} \frac{b_j}{d_0} \frac{l_e}{d_0}; \quad K_n = \left[\frac{(\omega_{g0} \cos \alpha_r - \omega_{q0})^2}{(\omega_{q0} \cos \alpha_r)^2} + \frac{(\omega_{g0} \sin \alpha_r)^2}{(\omega_{q0} \sin \alpha_r)^2} \right].$$

The quantity ε_f characterizes the relative transverse deformation of the contour of the jet by the flow. The simplex ε_n is the product of the dimensionless atomization surface $(b_j/d_0)(l_e/d_0)$ and the ratio of the densities on the one hand and the bending coefficient K_n on the other hand. For the given jet trajectory, $K_n \approx \text{const}$ with a fixed value of ω_{g0}.

In the first case, the dependent of f_b; F/F_0, and ΔM on ε_f was connected with the extreme character of the surface tension of the liquid and the gas flow at the edges of the jet as it was being flattened. The correlation between these quantities and ε_n in the second case was due to the dominant effect of the flexural deformation (the value of φ) and ω_{g0} on the breakdown of the jet, allowance being made here for the fact that $\omega_{g0} \gg \omega_{q0}$ (Fig. 2). The photographs and films showed that bending of the core created a complex system of folds, waves, projections, and capillary undulations on its surface. These features were stripped away by the gas flow, thus forming "trails" and a cloud of droplets that transformed the core [21, 25]. At $\varphi \geq 0.6$ and $\omega_{g0} > 60$ m/sec, when the jet was bent at the edge of the orifice, the droplet cloud became attached to the root of the jet near the mouth. The deformation of the jet from the pressure associated with the dynamic head of the gas prepared its surface for atomization. Such a disintegration mechanism can be referred to as deformational. Deformation precedes the collapse of the surface perturbations, but it is deformation that determines the trajectory of the jet, i.e., the trajectory is determined by the flattening or flexure of the jet [24, 44]. This helps explain the above-noted independence of penetration on the degree of breakdown and the one-sided character of the effect of the trajectory on breakdown. Data on the length, deformation [25], and velocity of the core of the jet leads to the conclusion that

$$\tau_{bj} > \tau_d \approx \tau_{df} + \tau_{dn}.$$

The mechanism described above is stagelike. Particular conditions of jet-flow interaction which upset the stagelike character of the mechanism lead to trajectory anomalies in which the dependence on φ is disturbed. The phenomenon of wave injection is one example [27, 28].

Values of $F_b = r_s/r_0$ were obtained from measurements performed in accordance with a transverse scheme with the use of two insulated needle-type probes having electrocontact areas in the region of the axis of the spray. The measurements were made below the core disintegration point. Despite the complexity of the phenomena taking place in the gap between the electrodes (see Fig. 1), the spray disintegration function F_b qualitatively characterizes the extent of its breakdown (erosion). The data in Fig. 4a shows that, after breakdown, the jet forms a dense ("rigid") spray which is subsequently diffused by the flow. The likelihood of the existence of such an intermediate structure was discussed in [45], but the present study is the first to offer empirical proof of its existence. As for the core of the jet, the approach of F_b toward infinity was taken as evidence of the erosion of the spray. The disintegration of the spray occurred much more rapidly than the disintegration of the core of the jet. For the cases we investigated, on the average $\tau_{bj}/\tau_{bs} \approx 3$, i.e., the total time of preparation of the fuel mixture consists for the most part of the time of atomization of the jet itself. The question of the mechanisms responsible for the disintegration of a dense spray is very complicated, due to the increasing role of turbulent pulsations and eddies that entrain drops from the spray. However, the curves (Fig. 4a), in combination with the ratio $j_{sx}/j_{jx} = 2$-7, provide the most likely hypothesis on the elongation of a "rigid" spray due to its acceleration. In any case, such deformation predominates. The acceleration and the density of the structure also evidently explain the fact that waves with increased length and amplitude but with diffuse contours sometimes continue to be generated on the surface of the spray. The rapid intensification of instability on such a small section — where a/d_0 reaches 1.5-2.5 and λ/d_0 reaches 3.5-4.5 — is connected with an increase in the number B_b. The latter is estimated here to increase to $(3\text{-}8)\cdot10^4$. The formation of an even larger wave ("fan") [23, 27, 28] is the limiting case of wave instability and is due to catastrophic disintegration of the core.

Processes which take place near the mouth are shown in Fig. 4b. Measurements made with a miniature probe having a diameter of 0.3 mm revealed a primary breakdown mechanism not encountered in the fragmentation of drops. This mechanism owes its existence to the act of discharge from the orifice and entails separation of the layer of liquid adjacent to the walls of the hole. It acts only over a short range, due to the zero velocity resulting from the deformation of the velocity profile in the short hole $(l/d_0)_q = 3.5$. This smooth laminar layer is stripped from the root of the jet in the entraining flow and breaks up into very fine drops which form a thin homogeneous sheath in the heated flow [22]. Analysis of the experimental data by the method described in [21] showed that $\Delta M = 0.05$-0.1 in this case. These values are greater than for a jet discharged into a submerged space. In the latter case, separation of the laminar sheath is realized through the development of a "wave ripple." A lengthwise distance corresponding to several jet diameters is needed for such a development to occur.

The authors of [1, 2, 7, 8, 11] paid particular attention to the mechanism of the "stripping" of a film from a slightly deformed liquid surface. For the case we studied, such stripping was seen only when the cylindrical part of the root of the jet was sufficiently long (curves 2 and 3 in Fig. 4b). An indication that such a situation exists is an increase in f_b with an increase in ω_{g0}. As described above, the intensification of bending at the same gas velocities leads to complex perturbations of the surface and changes the disintegration process over to control by the deformational mechanism, beginning from the mouth (curves 4 and 5 in Fig. 4b).

The studies [1, 2, 4, 6] made it possible to formulate the main principle underlying the breakup of drops (jets). In accordance with this principle, the process occurring at the highest rate (having the shortest characteristic time) determines the fragmentation rate and becomes the disintegration mechanism. For a low-viscosity jet in a subsonic entraining flow of gas, the main variant of disintegration from the mouth to assimilation of the "rigid" spray by the flow is the deformational variant, i.e., fragmentation of a flattened and bent core, separation of a laminar sheath near the mouth, or erosion of a dense droplet spray. None of the disintegration phenomena develop more rapidly than the deformational effects on which they are based. This fact accounts for the stagelike character of the breakdown. Significant forcing of the deformational processes leads to catastrophic disintegration regimes [23, 27, 28]. The deformational mechanisms can be influenced by changing the atomization and mixing rates.

The core of the jet remained intact, despite the jumps in f_b near the jet's disintegration point and near the mouth (see Fig. 2 and Fig. 4b). As was shown by the optical and electrocontact measurements, such a flow model becomes invalid on the dense-spray section. Here, discontinuities develop at a frequency of 100-300 Hz. The model is similar to the Schetz scheme [14-17], but in contrast to the latter it attributes these discontinuities to the separation of accelerating sections of the rigid spray. These sections accumulate below the core disintegration point (see Fig. 1).

It must also be noted that the main laws governing fragmentation depend slightly on the temperature of the gas. This dependence only affects the vaporization (combustion) of already-atomized fuel; the basic structure of the jet, the trajectory, and the mechanisms of its disintegration remain unchanged [1, 5, 17, 24]. Thus, the information obtained under cold conditions makes it possible to perform electrocontact measurements suitable for predicting processes occurring in reactive gas—liquid flows. Proof of this is the physical model of flame stabilization obtained in [22] on the basis of data from electrocontact probing of the root of a jet atomized by a cold air flow.

Conclusion. The use of the electrocontact method as the main method of investigation has made it possible to establish the stagelike character and leading mechanisms of jet disintegration. A model based on the deformational mechanism generalizes all stages of the disintegration. The laws that were established make it possible to control disintegration phenomena in order to improve the combustion of liquid fuels.

NOTATION

Here f_b is the jet breakdown function; R_j, resistance of the jet undergoing disintegration; R_0, resistance of the intact jet, with the length l_e from the mouth to the probe installation point reckoned along the external boundary of the jet; ρ_q, resistivity of water; F_0, area of the hole for injection of the jet; F, running cross-sectional area of jet undergoing disintegration; ρ_g, density of the gas; ρ_q, density of the liquid; ω_{g0}, velocity of the entraining gas flow; ω_{q0}, liquid discharge velocity; φ, simplex of ratio of the dynamic head of the gas to the dynamic head of the liquid; $\angle\alpha_0$, initial angle of injection into the flow; $\angle\alpha_r$, running angle along the injection line; $(l/d_0)_q$, ratio of the length of the discharge hole to its diameter d_0; a, λ, amplitude and length of wave on the front surface of the jet; p, T, static pressure and temperature of the gas; j_{jx}, j_{sx}, axial accelerations of the jet and spray, respectively; B, Bond number; W, Weber number; σ, surface tension of liquid; b_j, jet propagation width; ε_f, ε_n, simplexes of flattening and flexural deformations; X/d_0, Y/d_0, coordinates of the trajectory of the external boundary of the jet; F_b, breakdown function of a dense spray; r_s, resistance of electrode gap during motion of the probe on the dense-spray section; r_0, resistance of the gap near the core disintegration point; τ_{bj}, τ_{bs}, times of disintegration of the jet and the spray, respectively; τ_d, time of deformation of the core; τ_{df}, τ_{dn}, times of deformation by flattening or bending; ΔM, fraction of liquid mass entrained from the surface of the jet. Indices: 0, initial parameters; g, gas; q, liquid; j, jet; s, spray; b, breakdown; eb, external boundary of jet.

LITERATURE CITED

1. S. M. Kogarko, B. E. Gel'fand, S. A. Gubin, and A. A. Borisov, Dokl. Akad. Nauk SSSR, **198**, No. 1, 71-73 (1971).
2. A. A. Borisov, B. E. Gel'fand, M. S. Natanzon, and O. M. Kossov, Inzh.-Fiz. Zh., **40**, No. 1, 64-70 (1981).
3. M. S. Volynskii, Dokl. Akad. Nauk SSSR, **68**, No. 2, 237-240 (1949).
4. B. E. Gel'fand, S. A. Gubin, and S. M. Kogarko, Inzh.-Fiz. Zh. **27**, No. 1, 119-126 (1974).
5. B. E. Gel'fand, S. A. Gubin, S. M. Kogarko, and S. P. Komar, Dokl. Akad. Nauk SSSR, **206**, No. 6, 1313-1316 (1972).
6. A. A. Borisov, B. E. Gel'fand, A. N. Polenov, et al., Izv. Akad. Nauk SSSR, Mekh. Zhidk. Gaza, No. 1, 165-168 (1986).
7. Ranger and Nichols, AIAA J., **7**, No. 2, 113-119 (1969).
8. O. G. Engel, J. Res. Nat. Bur. Stand., **60**, No. 3, 245-280 (1958).
9. E. I. Harper, G. W. Crube, and I. D. Chang, J. Fluid Mech., **52**, Pt. 3, 565-591 (1972).
10. P. G. Simpkins, "On the distortion and breakup of suddenly accelerated droplets," AIAA Paper, No. 321 (1971).
11. A. A. Buzukov, Zh. Prikl. Mekh. Tekh. Fiz., No. 2, 154-158 (1963).
12. M. Adelberg, AIAA J., **5**, No. 3, 40-48 (1967).
13. E. A. Kush and I. A. Schetz, "Liquid injection into a supersonic flow," AIAA Paper, No. 1180 (1972).
14. I. Schetz, E. A. Kush, and P. B. Joshi, AIAA J., **18**, No. 7, 191-198 (1980).
15. A. S. Nejad and I. A. Schetz, "The defects of viscosity and surface tension of liquid injectants on the structural characteristics of the plume in a supersonic airstream," AIAA Paper, No. 253 (1982).
16. A. S. Nejad and I. A. Schetz, AIAA J., **22**, No. 4, 458-459 (1984).
17. I. A. Schetz, P. W. Hewitt, and M. Situ, AIAA J., **23**, No. 4, 596-603 (1985).
18. D. M. Less and I. A. Schetz, AIAA J., **24**, No. 12, 1979-1986 (1986).
19. Schetz and Podhai, AIAA J., **15**, No. 10, 13-21 (1977).
20. B. I. Clark, "Break up of a liquid jet in a transverse flow of a gas," NASA Tech. Note, No. 2424 (1964).
21. M. E. Rudyak, Izv. Vyssh. Uchebn. Zaved., Aviats. Tekh., No. 3, 32-38 (1983).
22. M. E. Rudyak, Fiz. Goreniya Vzryva, **22**, No. 5, 70-75 (1986).
23. M. E. Rudyak, Izv. Vyssh. Uchebn. Zaved., Aviats. Tekh., No. 1, 42-46 (1986).
24. M. E. Rudyak, Izv. Vyssh. Uchebn. Zaved., Aviats. Tekh., No. 6, 60-64 (1988).
25. M. E. Rudyak, Izv. Vyssh. Uchebn. Zaved., Aviats. Tekh., No. 4, 90-92 (1987).
26. M. E. Rudyak, Fiz. Goreniya Vzryva, **19**, No. 3, 77-81 (1983).
27. M. E. Rudyak, Izv. Vyssh. Uchebn. Zaved., Aviats. Tekh., No. 1, 110-112 (1983).

28. "Device for dispersing liquid with a gas and mixing them," Inventor's Certificate No. 1212535 SSSR. Mkl4 BOIF 5/18.
29. R. A. Castleman, J. Res. Nat. Bur. Stand., **6**, No. 3, 369-376 (1931).
30. D. W. Lee and R. Spenser, Internal Combustion Engines [Russian translation], Vol. 1, Moscow—Leningrad (1936), pp. 139-168.
31. Harvey, AIAA J., **11**, No. 6, 73-78 (1973).
32. N. S. Panasenkov, Zh. Tekh. Fiz., **21**, No. 2, 160-166 (1951).
33. L. F. Vereshchagin, A. A. Semerchan, and S. S. Sekoyan, Zh. Tekh. Fiz. **29**, No. 1, 45-50 (1959).
34. T. F. Chen and J. R. Davis, Agric. Eng., **42**, No. 4, 27-28 (1961).
35. T. F. Chen and I. R. Davis, Proc. Am. Soc. Civ. Eng., **90** NOHY1, Pt. 1, 175-206 (1964).
36. E. Ralph Phinney, AIChE J., **21**, No. 5, 996-999 (1975).
37. V. Yu. Nezgada, Izv. Akad. Nauk SSSR, Mekh. Zhidk. Gaza, No. 4, 151-155 (1970).
38. M. Wicks and A. Dakler, Advances in Heat Transfer [Russian translation], Moscow (1970), pp. 170-187.
39. V. D. Vorontsov, Teplofiz. Vys. Temp., **14**, No. 3, 568-573 (1976).
40. G. G. Bartolomei and V. A. Solodkii, Tr. Mosk. Energ. Inst. (Thermohydraulic and Physicochemical Processes in Nuclear Power Plants), No. 328, 20-24 (1977).
41. E. G. Bratuta and A. R. Pereselkov, Énergomashinostroenie, **16**, 72-78 (1973).
42. J. J. Picot, T. D. Tomey, I. B. Smidley, and D. D. Kristmanson, Can. J. Chem., **58**, No. 3, 314-317 (1980).
43. I. O. Hinze, AIChE J., **1**, No. 3, 289-295 (1955).
44. B. V. Raushenbakh, S. A. Belyi, I. V. Bespalov, et al., Physical Principles of Combustion in Jet Engines [in Russian], Moscow (1964).
45. I. V. Astakhov, V. I. Trusov, A. S. Khachiyan, and L. N. Golubkov, Feed and Atomization of Fuel in Diesels [in Russian], Moscow (1972).
46. I. M. Hoyt and I. I. Taylor, Phys. Fluids (Proceed. Intern. Symp. on Structure of Turbulence and Drag Reduction), **20**, No. 10, Pt. 11, 253-257 (1977).
47. I. M. Hoyt and I. I. Taylor, J. Fluid Eng., **101**, No. 3, 304-308 (1979).